Area selective deposition of silicon by plasma enhanced chemical vapor deposition using a fluorinated precursor

Ghewa Akiki, Daniel Suchet, Dmitri Daineka, Sergej Filonovich, Pavel Bulkin, Erik Johnson

Applied Surface Science 531 (2020) 147305

Contents lists available at ScienceDirect

Applied Surface Science

journal homepage: www.elsevier.com/locate/apsusc

Area selective deposition of silicon by plasma enhanced chemical vapor deposition using a fluorinated precursor

Ghewa Akiki[a,*], Daniel Suchet[a], Dmitri Daineka[a], Sergej Filonovich[b], Pavel Bulkin[a], Erik V. Johnson[a]

[a] Laboratoire de Physique des Interfaces et des Couches Minces, CNRS, Ecole Polytechnique, Institut Polytechnique de Paris, 91128 Palaiseau, France
[b] TOTAL GRP, 2 Place Jean Millier – La Défense 6, 92078 Paris La Défense Cedex, France

ARTICLE INFO

Keywords:
Area selective deposition
PECVD
Microcrystalline silicon
Silicon tetrafluoride
AlO_x
SiN_x

ABSTRACT

An Area Selective Deposition (ASD) process using Plasma-Enhanced Chemical Vapour Deposition (PECVD) is demonstrated. Using a plasma chemistry containing a fluorinated silicon precursor (SiF_4), no deposition is observed on an aluminum oxide (AlO_X) surface area, whereas a thin film of silicon is deposited on a silicon nitride (SiN_X) surface area, while both areas are located on the same crystalline silicon substrate. The thin film deposition is characterized using spectroscopic ellipsometry, scanning electron microscopy, and atomic force microscopy, showing that 10 nm of silicon is deposited on the SiN_x in 4 min. The growth on the SiN_X is characterized by small grains and a rough surface, consistent with microcrystalline silicon, while no deposition or etching is observed for the AlO_X surface.

1. Introduction

Area selective deposition (ASD) is an attractive process for applications such as microelectronics as it may eliminate some costly lithography steps and reduce the issue of edge placement errors [1]. This bottom-up approach controls where deposition takes place through the underlying surface rather than through any masking step, and results in "growth" and "no-growth" areas depending on the nature of surface material.

Recent research in this field predominantly employs two techniques: atomic layer deposition (ALD) and self-assembling monolayers (SAMs). In the ALD technique, for certain precursors, the nucleation delay before the start of growth depends strongly on the surface properties. However, this nucleation delay appears only at the first stage of the growth process and for a relatively short time [2]. R. Vallat et al. have demonstrated the inclusion of a plasma etching step to Plasma Enhanced ALD (PEALD) to "reset" the nucleation delay on the no-growth area. Doing so, a super cycle of deposition and etching processes are repeated until the desired thickness is reached on the growth area [3]. Alternatively, one can introduce a surface-selective SAM on the no-growth surface in order to deactivate it and prevent growth [4–6] or to form a seed layer to catalyze and promote deposition on the growth area [7].

Area selective deposition has been observed for other growth technologies as well. For example, the selective deposition of tungsten by chemical vapor deposition (CVD) has been demonstrated using an oxide masked area on a silicon substrate [8]. For lower temperature plasma enhanced CVD (PECVD), selective deposition has been observed when using pulsed gas plasmas [9].

In this paper, we report on the observation of a significant surface-dependent nucleation delay in the PECVD of hydrogenated microcrystalline silicon (μc-Si:H) films using a standard 13.56 MHz radio frequency excitation source and a fluorinated silicon growth precursor.

2. Experimental details

The μc-Si:H deposition process used is a RF-PECVD technique in a capacitively-coupled plasma (CCP) chamber [10] using a $SiF_4/H_2/Ar$ gas mixture. Samples were placed on the grounded electrode, and the temperatures of the grounded and powered electrodes were both kept at 150 °C. The inter-electrode distance was 22 mm, and the SiF_4, H_2 and Ar flows were 7, 9 and 100 sccm, respectively, with a pressure of 2.3 Torr and a power of 15 Watts. A similar plasma chemistry has been recently utilized to make high-quality thin film solar cells [11], and, using Tailored Voltage Waveforms as the excitation source, to demonstrate the electrode selective deposition of μc-Si:H [12]. For this study, a process time of 4 min was used. The selectivity is not affected by process time but rather by H_2 gas flow, plasma power, electrode and

* Corresponding author.
E-mail address: ghewa.akiki@polytechnique.edu (G. Akiki).

https://doi.org/10.1016/j.apsusc.2020.147305
Received 26 March 2020; Received in revised form 16 July 2020; Accepted 17 July 2020
Available online 27 July 2020

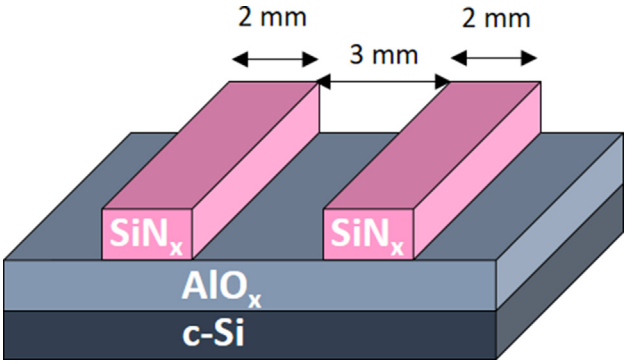

Fig. 1. Schematic presentation of AlO_x/SiN_x patterned sample.

substrate holder temperatures, and substrate type.

The substrates for deposition consisted of a silicon wafer (with native oxide) coated with the following:

1) 50 nm of AlO_x by Picosun ALD deposited using TMA and water as precursors (500 ALD cycles).
2) 200 nm of SiN_x deposited by capacitively coupled-PECVD, using N_2 and SiH_4 gases.
3) AlO_x/SiN_x patterned samples (Fig. 1) were then fabricated by photolithography employing Reactive Ion Etching (RIE). 30 sccm of SF_6 gas flow, 20 W of RF power and a pressure of 30 mTorr were used to etch selectivity the SiN_x area not covered by MEGAPOSIT SPR700 1.2 positive photoresist. The remaining photoresist is removed by acetone and the sample is then immersed in isopropanol.

Ex-situ spectroscopic ellipsometry (UVISEL-1 by Horiba Jobin Yvon) was performed (in a spectral range from 1.2 to 4.5 eV) on both AlO_x and SiN_x areas, before and after the process. The SE spectrum was fitted to a model using DeltaPsi2 software. This model is built as follow: first the substrate layers were measured and modelled (consisting of a crystalline silicon substrate with a 50 nm layer of AlO_x and a 200 nm layer of SiN_x) before any plasma exposure. The thicknesses of those layers were fixed for the modeling after plasma exposure and only the thickness as well as the optical constants of the deposited material are allowed to vary and be fitted. Scanning electron microscopy (SEM) observations of the deposited film were carried out on a HITACHI S-4800 microscope with a field emission source at 10 kV and 5 μA (using the upper detector). Atomic Force Microscopy (AFM) measurements were done using an Aglient Technologies 5500 Scanning Probe Microscope with lateral and vertical resolutions of 10 nm and 0.5 nm, respectively, in Intermittent Contact or Alternating Current mode (ACAFM).

3. Results and discussion

Ellipsometry measures the change of polarization state of a light beam caused by reflection on a sample. This change of polarization is represented by the ellipsometric angles Δ and Ψ [13,14]. Fig. 2 presents the ex-situ spectroscopic ellipsometry spectra measured on both the SiN_x and the AlO_x areas of the patterned substrate. Filled symbols indicate the ellipsometric spectra acquired before exposing the substrate to the deposition plasma for 4 min, whereas, open symbols indicate the ellipsometric spectra acquired after plasma exposure. A clear change in the spectra is observed only for the SiN_x area (Fig. 2a), while the spectrum for the AlO_x area (Fig. 2b) remains unchanged. Furthermore, in Fig. 2a, the shift of the interference peaks towards lower photon energy clearly indicates that a deposition process has occurred on top of the SiN_x area.

In order to quantify the change in the spectra observed for the SiN_x area, the SE spectrum was modelled. The post-deposition model used, unchanged, the model of the substrate stack before any plasma exposure (a crystalline silicon substrate with a 50 nm layer of AlO_x and a 200 nm layer of SiN_X). The material deposited on top of the stack is modelled with a Tauc-Lorentz dispersion function. This generic dispersion curve is usually reserved for amorphous films at greater thicknesses, but can be used for microcrystalline silicon when the layers are very thin [15,16].

A schematic presentation of the model is given in Fig. 3, where the AlO_x and SiN_x thicknesses are fixed, while the optical constants of the silicon layer as well as the thickness are fitted. The deposited layer has a thickness of 12 nm and appears to be of rather low density, as indicated by the low refractive index of the material provided by the model.

To directly observe the nature of the growth that is occurring on the SiN_x, SEM images of the AlO_x and SiN_x areas of the patterned substrate were acquired and are presented in Fig. 4. The SiN_x area is completely covered with densely packed grains of about 60 nm in diameter. However, on the AlO_x area there is a negligible amount of nuclei, particularly in comparison to the SiN_x area. The morphology of the growth on the SiN_X area, with a high roughness and small dense grains, is consistent with μc-Si:H growth.

To quantify the roughness of the films deposited, AFM measurements were performed on SiN_x and AlO_x areas. The RMS surface roughness was calculated for each area. For the SiN_x area it is 4.5 nm while for the AlO_x area is 1.4 nm. The significance of the value for the AlO_X area is debatable, as this incorporates the effect of the few sparse nuclei that are present. However, the RMS roughness for the SiN_X area corroborates the modelling performed by SE.

The measurements presented above unequivocally demonstrate the selective deposition of a silicon layer on a SiN_x surface while leaving an AlO_x area pristine, both while using the same $Ar/SiF_4/H_2$ PECVD process. For the SiN_x area, modelling of the shift in the ellipsometry spectra before and after deposition indicate the growth of a layer about 10 nm thick, as confirmed by SEM and AFM measurements. Furthermore, the unchanged ellipsometry spectra for the AlO_x before and after the plasma (Fig. 2b) indicate that the plasma did not significantly modify the structure of AlO_x, and that no etching occurred. The importance of the few nuclei observed on the AlO_X surface is not clear; no special care was taken to keep the substrate ultra-clean, so these may simply be the consequence of dust particles.

The physical origin of this PECVD ASD phenomenon is not yet clear, but the experimental design eliminates some possibilities. Firstly, the fact that the two growth areas are located on the same c-Si substrate means the two areas are at the same temperature, and once in the plasma, will be at the same potential relative to the plasma [17,18]. The fact that one area cannot charge up more than the other (as could occur if one substrate was insulating and the other conductive [19]) means that the ion flux profile seen by the two surfaces should be very similar.

One is then left to consider whether this ASD effect is due to local differences in the plasma chemistry or in the surface chemistry. Globally, this specific SiF_4/H_2 plasma chemistry is believed to be a key ingredient in creating this nucleation delay, as the processes on the surface (deposition vs etching) are strongly determined by the H_2 flow rate. In fact, it has been shown that silicon deposition will only occur if the H_2 flux is sufficient to scavenge the fluorine (resulting from the dissociation of SiF_4) through the formation of HF molecules. For insufficient H_2 feed flow, the fluorine concentration remains too high, and the plasma will etch any silicon that is present [20].

One possibility for the selectivity between the two surfaces is that the plasma, very locally, is different due to some influence from the surface, such as different secondary electron emission properties or molecular recombination rates. If this were the case, however, one would expect a more gradual transition in nucleation rate at the boundary between the two surfaces, which is not the case [21].

A second possibility is that the precursors involved in the process (either SiF_x, F or H) react with the two surface areas in different ways. A fluorination reaction occurring on AlO_x area forms a very strong bond (Al-F) that blocks etching or deposition on this area. In the contrary,

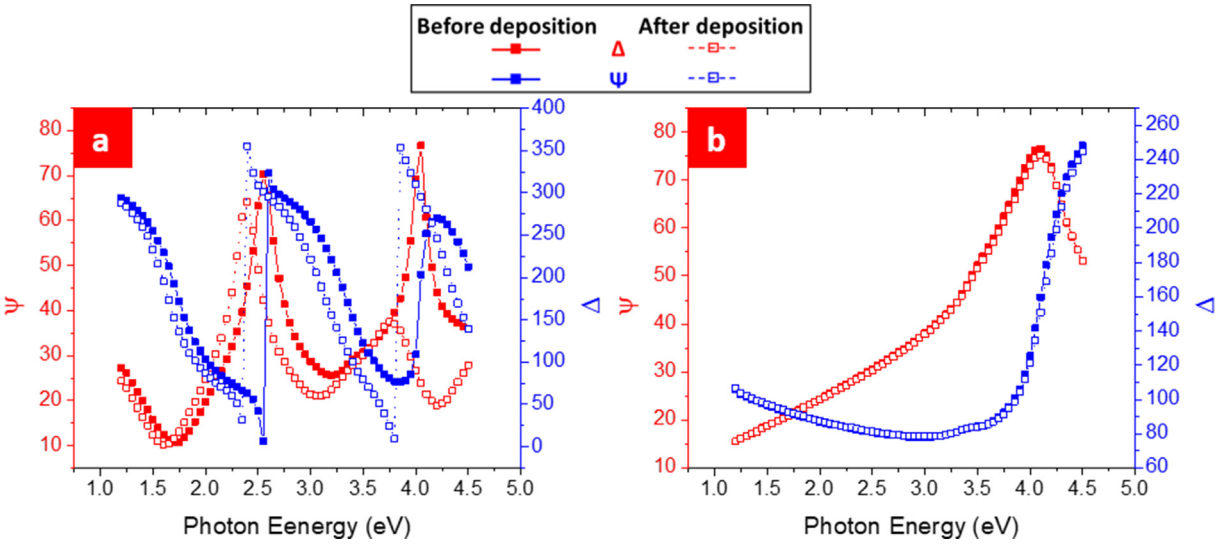

Fig. 2. Comparison of ellipsometry spectra for (a) SiN_x and (b) AlO_X covered areas on the same SiN_x/AlO_x patterned substrate before (filled symbols) and after (open symbols) the plasma process.

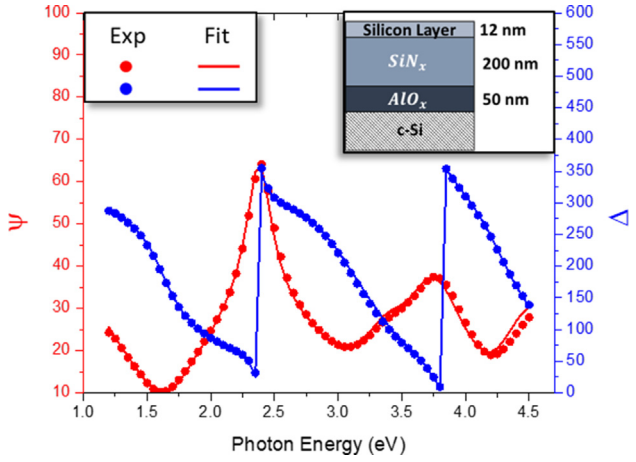

Fig. 3. Ellipsometric spectra for silicon layer deposited on top of Silicon Nitride (SiN_x) area represented by Blue and Red circles. Solid lines show the fitting spectra from the optical model of the substrate present on the right.

plasma species create volatile or gaseous compounds when reacting on SiN_x surface area that are removed easily from the surface, leaving sites where growth can nucleate [22,23]. The influence of fluorine on selective deposition has been previously shown [24], where Si–F bonds passivate silicon substrates from TiO_2 growth and block surface reactions. Such processes appear to be likely explanations for the effect observed, but need to be directly confirmed by advanced surface analysis techniques such as X-ray Photoelectron Spectroscopy (XPS).

4. Conclusions

The selective, low temperature growth of silicon by PECVD, depositing on SiN_X while leaving an adjacent AlO_X area pristine, has been unambiguously demonstrated through spectroscopy ellipsometry (SE) and scanning electron microscopy (SEM). The SE results show that the silicon layer that has grown on the SiN_X area can be optically modelled as a continuous thin film (although one of low density), and that optically, no difference can be detected in the AlO_X region before and after the process (no growth, etching, or roughening). The SEM results show the details of the morphologies of the two surfaces; the growth on the SiN_X area is indeed a continuous film with a rough, grain-like surface, while the AlO_X area shows very sparse features that are below the measurement capabilities of the SE.

The characterization techniques used in this study do not provide a clear underlying physical explanation for the growth selectivity. However, the experimental design and the results of characterization can be used to ***eliminate*** some possible explanations. For example, both surfaces being adjacent and on the same substrate indicates that the selectivity ***cannot*** be caused by a difference in ion flux profile, nor by

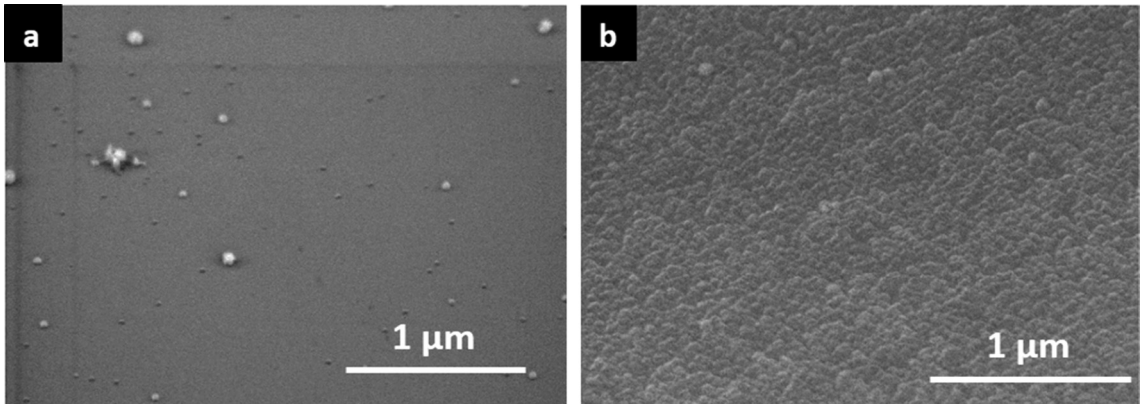

Fig. 4. A top view SEM images of (a) AlO_X and (b) SiN_X area. Only a few sparse features are observable on the AlO_x area, while many small grains cover the SiN_x area. The presence of these grains is related to the microcrystalline nature of the deposited film.

local differences in the plasma, caused (for example) by a difference in secondary electron emission coefficient. In light of this evidence, we suspect that the SiF_4 precursor used to grow the silicon layers plays an important role, and specifically that the fluorine generated from its dissociation is behind the selectivity. Nevertheless, determining the most likely explanation (namely, a surface-related effect preventing the sequence of elementary steps necessary for growth) requires more experimental evidence to narrow down the exact process.

CRediT authorship contribution statement

Ghewa Akiki: Writing - original draft, Writing - review & editing, Investigation. **Daniel Suchet:** Investigation. **Dmitri Daineka:** Investigation. **Sergej Filonovich:** Supervision, Project administration. **Pavel Bulkin:** Investigation, Supervision, Writing - original draft, Writing - review & editing. **Erik V. Johnson:** Writing - review & editing, Writing - original draft, Supervision, Project administration, Funding acquisition.

Declaration of Competing Interest

The authors declare that they have no known competing financial interests or personal relationships that could have appeared to influence the work reported in this paper.

Acknowledgment

This activity is funded through the Total-LPICM ANR Industrial Chair “PISTOL” (Contract ANR-17-CHIN-0002-01).

References

[1] J. Mulkens, M. Hanna, B. Slachter, W. Tel, M. Kubis, M. Maslow, C. Spence, V. Timoshkov, D. Run, N.W. Everygreen, P. Hillsboro, Patterning control strategies for minimum edge placement error in logic devices (2017) 10145.
[2] A.J.M. Mackus, A.A. Bol, W.M.M. Kessels, The use of atomic layer deposition in advanced nanopatterning, Nanoscale 6 (2014) 10941–10960.
[3] R. Vallat, R. Gassilloud, B. Eychenne, C. Vallée, Selective deposition of Ta 2 O 5 by adding plasma etching super-cycles in plasma enhanced atomic layer deposition steps, J. Vac. Sci. Technol. A 35 (2017) 01B104.
[4] R. Chen, H. Kim, P.C. McIntyre, D.W. Porter, S.F. Bent, Achieving area-selective atomic layer deposition on patterned substrates by selective surface modification, Appl. Phys. Lett. 86 (2005) 1–3.
[5] X. Jiang, S.F. Bent, Area-selective ALD with soft lithographic methods: Using self-assembled monolayers to direct film deposition, J. Phys. Chem. C 113 (2009) 17613–17625.
[6] S. Seo, et al., Reaction mechanism of area-selective atomic layer deposition for Al_2O_3 nanopatterns, ACS Appl. Mater. Interfaces 9 (47) (2017) 41607–41617.
[7] J.A. Singh, N.F.W. Thissen, W.H. Kim, H. Johnson, W.M.M. Kessels, A.A. Bol, S.F. Bent, A.J.M. MacKus, Area-selective atomic layer deposition of metal oxides on noble metals through catalytic oxygen activation, Chem. Mater. 30 (3) (2018) 663–670.
[8] J. Carlsson, M. Boman, Selective deposition of tungsten—prediction of selectivity, J. Vac. Sci. Technol. A 3 (1985) 2298–2302.
[9] G.N. Parsons, J.J. Boland, J.C. Tsang, Selective deposition and bond strain relaxation in silicon PECVD using time modulated silane flow, Jpn. J. Appl. Phys. 31 (1992) 1943–1947.
[10] P. Roca i Cabarrocas, J.B. Chévrier, J. Huc, A. Lloret, J.Y. Parey, J.P.M. Schmitt, A fully automated hot-wall multiplasma-monochamber reactor for thin film deposition, J. Vac. Sci. Technol. A 9 (1991) 2331–2341.
[11] J.C. Dornstetter, B. Bruneau, P. Bulkin, E.V. Johnson, P. Roca I Cabarrocas, High efficiency thin film solar cells deposited at the amorphous-tomicrocrystalline transition using SiF4/H2/Ar gas mixtures, 2014 IEEE 40th Photovolt. Spec. Conf. PVSC 2014, 2014, pp. 2839–2841.
[12] J.K. Wang, E.V. Johnson, Electrode-selective deposition/etching processes using an SiF4/H2/Ar plasma chemistry excited by sawtooth tailored voltage waveforms, Plasma Sources Sci. Technol. 26 (2017) 01LT01.
[13] H. Fujiwara, Spectroscopic Ellipsometry: Principles and Applications, John Wiley & Sons, 2007.
[14] H.G. Tompkins, E.A. Irene, Handbook of Ellipsometry, William Andrew, 2005.
[15] G.E. Jellison Jr., V.I. Merkulov, A.A. Puretzky, D.B. Geohegan, G. Eresa, D.H. Lowndes, J.B. Caughman, Characterization of thin-film amorphous semiconductors using spectroscopic ellipsometry, Thin Solid Films 377–378 (2000) 68.
[16] G.E. Jellison, F.A. Modine, Parameterization of the optical functions of amorphous materials in the interband region, Appl. Phys. Lett. 69 (1996) 371–373.
[17] K.S. Sree Harsha, Principles of Vapor Deposition of Thin Films, Elsevier, 2005 Chapter 4.
[18] Wilfried G.J.H.M. Van Sark, Methods of deposition of hydrogenated amorphous silicon for device applications, Thin Films and Nanostructures, vol. 30, Academic Press, 2002.
[19] J. Cazaux, Recent developments and new strategies in scanning electron microscopy, J. Microsc. 217 (2005) 16–35.
[20] J.C. Dornstetter, B. Bruneau, P. Bulkin, E.V. Johnson, P. Roca I Cabarrocas, Understanding the amorphous-to-microcrystalline silicon transition in SiF4/H2/Ar gas mixtures, J. Chem. Phys. 140 (2014).
[21] A.J. Dekker, Secondary electron emission, Solid State Phys. (1958) 251–311.
[22] K. Shinoda, M. Izawa, T. Kanekiyo, K. Ishikawa, M. Hori, Thermal cyclic etching of silicon nitride using formation and desorption of ammonium fluorosilicate, Appl. Phys. Express 9 (2016) 3–6.
[23] D. Humbird, D.B. Graves, Atomistic simulations of spontaneous etching of silicon by fluorine and chlorine, J. Appl. Phys. 96 (2004) 791–798.
[24] R. Vallat, R. Gassilloud, O. Salicio, K. El Hajjam, G. Molas, B. Pelissier, C. Vallée, Area selective deposition of TiO2 by intercalation of plasma etching cycles in PEALD process: a bottom up approach for the simplification of 3D integration scheme, J. Vac. Sci. Technol. A 37 (2019) 020918.